3374 *Organometallics* **2007,** *26,* 3374−3384

New Types of Constrained Geometry Group 4 Metal Complexes Derived from the Aminomethyldicarbollyl Ligand System: Synthesis and Structural Characterization of Mono-dicarbollylamino and Bis-dicarbollylamino Group 4 Metal Complexes

Jong-Dae Lee,[†] Young-Joo Lee,[†] Ki-Chul Son,[†] Minserk Cheong,[‡] Jaejung Ko,*[,†] and
Sang Ook Kang*[,†]

*Department of Chemistry, Korea University, 208 Seochang, Chochiwon, Chung-nam 339-700, Korea, and
Department of Chemistry and Research Institute for Basic Sciences, Kyung Hee University,
Seoul 130-701, Korea*

Received February 21, 2007

A series of constrained geometry group 4 metal complexes containing the (*N*,*N′*-dimethylaminomethyl) dicarbollyl ligand $\mathrm{Dcab}^{N}\mathrm{H}$ [*nido*-7-$\mathrm{NHMe_2(CH_2)}$-8-R-7,8-$\mathrm{C_2B_9H_{10}}$] (**3**) was prepared. New types of constrained geometry titanium complexes with the formula $\mathrm{(Dcab^{N})TiCl_2}$, $[\{(\eta^5\text{-}\mathrm{RC_2B_9H_9})(\mathrm{CH_2})(\eta^1\text{-}\mathrm{NMe_2})\}\mathrm{TiCl_2}]$ (R = H, **4a**; Me, **4b**), were produced by the reaction of the potassium salt of **3** with titanium tetrachloride. The reaction of **3** with $\mathrm{Ti(NMe_2)_4}$ in toluene afforded $\mathrm{(Dcab^{N})Ti(NMe_2)_2}$, $[\{(\eta^5\text{-}\mathrm{RC_2B_9H_9})(\mathrm{CH_2})(\eta^1\text{-}\mathrm{NMe_2})\}\mathrm{Ti(NMe_2)_2}]$ (**5**) (R = H, **a**; Me, **b**), which readily reacted with $\mathrm{Me_3SiCl}$ to yield the corresponding chloride complexes $\mathrm{(Dcab^{N})TiCl_2}$ (**4**). However, the reaction of **3** with $\mathrm{Zr(NMe_2)_4}$ in toluene afforded $\mathrm{(Dcab^{N})Zr(NMe_2)_2(HNMe_2)}$ $[\{(\eta^5\text{-}\mathrm{RC_2B_9H_9})(\mathrm{CH_2})(\eta^1\text{-}\mathrm{NMe_2})\}\mathrm{Zr(NMe_2)_2(HNMe_2)}]$ (**6**) (R = H, **a**; Me, **b**). The structures of the diamido complexes were established by X-ray diffraction studies of **5a** and **5b**, which authenticated an $\eta^5;\eta^1$-bonding mode derived from the dicarbollylamino ligand functional group. The corresponding bis-chelate complexes, $\mathrm{(Dcab^{N})_2Ti}$ (**7**), were synthesized from the reaction of **4a** with an additional dicarbollyl ligand **3a**. Bis-chelated complexes $\mathrm{(Dcab^{N})_2M}$ (M = Ti, **7**; Zr, **8**; Hf, **9**) were also formed upon the reaction of **3a** with $\mathrm{MX_4}$ (M = Ti, Zr, Hf) in a 2:1 molar ratio. The NMR spectra revealed that intramolecular M−N coordinations were preserved in solution, resulting in the formation of bis-chelated complexes $\mathrm{(Dcab^{N})_2M}$ (**7**−**9**). The tetrahedral coordination of the metal center was proven by single-crystal X-ray determination of the complex $\mathrm{(Dcab^{N})_2Zr}$ (**8**). New types of titanium alkoxides, $\mathrm{(Dcab^{N})Ti(O^{i}Pr)_2}$ (**10**), were synthesized from the reaction of **3a** with $\mathrm{Ti(O^{i}Pr)_4}$. Sterically less-demanding phenols such as $\mathrm{C_6H_5OH}$ and 2-$\mathrm{MeC_6H_4OH}$ replaced the coordinated amido ligands on $\mathrm{(Dcab^{N})Ti(NMe_2)_2}$ (**5a**) to yield the aryloxy-stabilized CGC complexes $\mathrm{(Dcab^{N})Ti(OPh)_2}$ (Ph = $\mathrm{C_6H_5}$, **11**; 2-Me-$\mathrm{C_6H_4}$, **12**). The NMR spectra suggested that an intramolecular Ti−N coordination was intact in solution, resulting in a stable piano-stool structure whereby two aryloxy ligands resided in the leg positions. The aryloxy coordinations were further confirmed by single-crystal X-ray diffraction studies on the complexes $\mathrm{(Dcab^{N})Ti(OPh)_2}$ (Ph = $\mathrm{C_6H_5}$, **11**; 2-Me-$\mathrm{C_6H_4}$, **12**).

Introduction

Much attention has been paid to constrained geometry catalysts based on the cyclopentadienyl-amido ligand due to their remarkable activity during the copolymerization of ethylene with α-olefins.[1] The sterically open nature of the catalyst center is believed to facilitate the incorporation of various α-olefins into growing polymer chains. As an extension of the structural variations[2] in the cyclopentadienyl derivatives of the group 4 metals, the dicarbollide moiety[3] has been employed as an η^5-coordinated group instead of the cyclopentadienyl (Cp) ligand. The dicarbollide ion is a versatile ligand and an isolobal inorganic analogue of the $\mathrm{Cp^-}$ ion. To prepare constrained geometry compounds with this dicarbollyl functionality is challenging because incorporation of dicarbollide fragments into ligand frameworks results in new metal/charge combinations. Therefore, recently developed constrained geometry complexes containing both π-dicarbollyl and σ-amino components have attracted considerable attention.[1] In fact, diverse reactivities associated with secondary interactions between metals and groups with an amino functionality have been observed. Amino tethers include monoamino dicarbollide systems containing either methylene-$\mathrm{(Dcab^{N})}$[4] or ethylene spacers $\mathrm{(Dcab^{EN})}$[5] and also the diamino functional ligand $\mathrm{(Dcab^{NN})}$[6] (Chart 1).

The formal replacement of a monoanionic $\mathrm{Cp^-}$ ligand in $[\mathrm{CpM(IV)}]^{3+}$ with an isolobal analogue, the dianionic ligand $\mathrm{(Dcab^{N})^{2-}}$, in the $[\mathrm{(Dcab^{N})M(IV)}]^{2+}$ fragment (Chart 1) reduces the overall charge by one unit but leaves the gross structural and metal frontier orbital properties unchanged. Similar dianionic ligands such as aminoborollide,[7] trimethylenemethane,[8] and diene[9] have been synthesized and converted into the corresponding group 4 metal complexes. Consequently, a potential advantage of catalyst designs of this type would be the control of secondary metal/ligand interactions. The weaker π-donating character and the lower steric requirements of the pendant neutral amino group enhance the metal's Lewis acidity by the simultaneous reduction of the formal electron count and by steric crowding at the electrophilic metal center. Thus, it

---

* Corresponding author. E-mail: sangok@korea.ac.kr.
[†] Korea University.
[‡] Kyung Hee University.

10.1021/om0701569 CCC: $37.00

Chart 1. Various Amino Group-Tethered CGC-Type Group 4 Metal Complexes

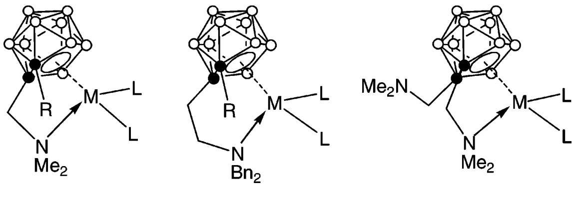

$\mathrm{Dcab}^{N}\mathrm{ML}_2$ $\mathrm{Dcab}^{EN}\mathrm{ML}_2$ $\mathrm{Dcab}^{NN}\mathrm{ML}_2$

was anticipated that incorporation of the dicarbollyl fragment into the CGC ligand framework would provide interesting opportunities for the design of complexes with new metal/charge combinations and increased metal unsaturation.

As part of our ongoing research into the utility of the aminoalkyldicarbollyl ligand in group 4 metal chemistry, we have published preliminary data on CGC complexes ($\mathrm{Dcab}^{N}\mathrm{TiCl}_2$) based on the aminomethyl dicarbollide ligand system.[4] Here, we give the full details of the synthesis, characterization, and polymerization activity of the aminomethyl dicarbollyl group 4 metal complexes, which involve η^5- and η^1-bound dicarbollyl-amino ligand systems (Dcab^{N}).

Scheme 1. Synthesis of Group 4 Metal CGC-Type Complexes Derived from the Aminomethyldicarbollyl Ligand 3[a]

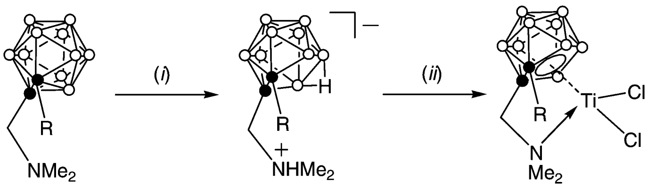

Cab^{N} **1** Dcab^{N} **3** $\mathrm{Dcab}^{N}\mathrm{TiCl}_2$ **4**

[a] Reagents and conditions: (*i*) (*a*) KOH, EtOH, 78 °C; (*b*) H_3PO_4, benzene, 25 °C, 10 h (R = H, **a**; CH_3, **b**). (*ii*) (*a*) KH, THF, 0 °C; (*b*) $TiCl_4$, toluene, −78 °C (R = H, **a**; CH_3, **b**).

Results and Discussion

We prepared a series of CGC-type group 4 metal complexes of the type $[\{(\eta^5\text{-}R^1C_2B_9H_{10})(CH_2)_n(\eta^1\text{-}NR^2_2)\}ML_2]$ (R^1 = H, Me; n = 1, 2; R^2 = Me, Bn; M = Ti, Zr; L = Cl, NMe_2) {-(Dcab^{N})ML_2,[4] (Dcab^{EN})ML_2,[5] (Dcab^{NN})ML_2)},[6] which involve η^5-dicarbollide and η^1-amine moieties. We observed that the stability of the desired CGC-type complexes increases in these ligand systems as the amino tether becomes bulkier. An example of such a bulky tether is the dibenzylamino group in ($\mathrm{Dcab}^{EN'}$)-ML_2. When two amino tethers were introduced, however, the amino pendant groups competed for coordination to the metal center, resulting in the formation of one-arm tethered CGC complexes instead of complexes with two-arm coordination. Study of the diamino-tethered complexes revealed the hemilabile character of the secondary metal−amino interaction in the aminodicarbollyl ligand system. In the present work, we have therefore focused on the coordination chemistry of less protected aminomethyl dicarbollyl ligands, in order to elucidate the thermodynamic driving force behind the formation of the CGC-type dicarbollide complexes (Dcab^{N})ML_2.

Ligand Synthesis. New (*N*,*N*′-dimethylaminomethyl)dicarbollyl ligands, abbreviated as Dcab^{N}H (**3**), were prepared by applying a standard deboronation procedure[10] to dimethylaminomethyl-*o*-carborane (*closo*-1-$NMe_2(CH_2)$-2-R-1,2-$C_2B_{10}H_{10}$) (R = H, **1a**; Me, **1b**) (Scheme 1). In this procedure, reaction of **1** with KOH in ethanol at 78 °C and subsequent protonation with phosphoric acid led to the formation of deboronated zwitterionic compounds **3**. An X-ray structural determination carried out on crystals produced by the cation exchange reaction revealed the formula *nido*-[7-$NMe_2(CH_2)$-8-R-7,8-$C_2B_9H_{10}]^-$-$[NMe_4]^+$ (**2a**). Figure 1 shows the conformation of the dimethylaminomethyl-tethered open dicarbollide structure of tetramethylammonium salts of **2a**; the availability of potential multidentate $\eta^5;\eta^1$-dicarbollylamino ligand functionalities can clearly be discerned in this structure.

Spectroscopic characterization of zwitterionic dicarbollyl ligands **3** showed that the dimethylamino group was linked to the *nido* cage carborane. The characteristic asymmetric pattern

---

(1) (a) McKnight, A. L.; Waymouth, R. M. *Chem. Rev.* **1998**, *98*, 2587. (b) Chen, Y.-X.; Metz, M. V.; Li, L.; Stern, C. L.; Marks, T. J. *J. Am. Chem. Soc*. **1998**, *120*, 6287. (c) Koo, K.; Marks, T. J. *J. Am. Chem. Soc*. **1998**, *120*, 4019. (d) Wang, W.; Yan, D.; Charpentier, P. A.; Zhu, S.; Hamielec, A. E.; Sayer, B. G. *Macromol. Chem. Phys*. **1998**, *199*, 2409. (e) Amor, F.; Butt, A.; du Plooy, K. E.; Spaniol, T. P.; Okuda, J. *Organometallics* **1998**, *17*, 5836. (f) Eberle, T.; Spaniol, T. P.; Okuda, J. *Eur. J. Inorg. Chem*. **1998**, 237. (g) Amor, F.; du Plooy, K. E.; Spaniol, T. P.; Okuda, J. *J. Organomet. Chem*. **1998**, *558*, 139. (h) Okuda, J.; Eberle, T. In *Metallocenes*; Halterman, R. L., Tongi, A., Eds.; Wiley-VCH: Weinheim, Germany, 1998; p 415. (i) Chen, Y.-X.; Fu, P.-F.; Stern, C. L.; Marks, T. J. *Organometallics* **1997**, *16*, 5958. (j) Mu, Y.; Piers, W. E.; MacQuarrie, D. C.; Zaworotko, M. J.; Young, V. G. *Organometallics* **1996**, *15*, 2720. (k) du Plooy, K. E.; Moll, U.; Wocadlo, S.; Massa, W.; Okuda, J. *Organometallics* **1995**, *14*, 3129. (l) Okuda, J.; Schattenmann, F. J.; Wocadlo, S.; Massa, W. *Organometallics* **1995**, *14*, 789. (m) Shapiro, P. J.; Cotter, W. D.; Schaefer, W. P.; Labinger, J. A.; Bercaw, J. E. *J. Am. Chem. Soc*. **1994**, *116*, 4623. (n) Canich, J. A. M. (Exxon) U.S. Patent 5,026,798, 1991. (o) Stevens, J. C.; Timmers, F. J.; Wilson, D. R.; Schmidt, G. F.; Nickias, P. N.; Rosen, R. K.; Knight, G. A.; Lai, S. Y. (Dow) Eur. Pat. Appl. 0416815 A2, 1991. (p) Fandos, R.; Meetsma, A.; Teuben, J. H. *Organometallics* **1991**, *10*, 59. (q) Okuda, J. *Chem. Ber*. **1990**, *123*, 1649. (r) Shapiro, P. J.; Bunel, E.; Schaefer, W. P.; Bercaw, J. E. *Organometallics* **1990**, *9*, 867.

(2) (a) Ashe, A. J., III; Fang, X.; Kampf, J. W. *Organometallics* **1999**, *18*, 1363. (b) Feng, S.; Klosin, J.; Kruper, W. J., Jr.; McAdon, M. H.; Neithamer, D. R.; Nickias, P. N.; Patton, J. T.; Wilson, D. R. *Organometallics* **1999**, *18*, 1159. (c) Brown, S. J.; Gao, X.; Harrison, D. G.; Koch, L.; Spence, R. E. v. H.; Yap, G. P. A. *Organometallics* **1998**, *17*, 5445. (d) Ashe, A. J., III; Al-Ahmad, S.; Fang, X.; Kampf, J. W. *Organometallics* **1998**, *17*, 3883. (e) de Boer, E. J. M.; Gilmore, I. J.; Korndorffer, F. M.; Horton, A. D.; van der Linden, A.; Royan, B. W.; Ruisch, B. J.; Schoon, L.; Shaw, R. W. *J. Mol. Catal. A: Chem*. **1998**, *128*, 155. (f) Rogers, J. S.; Bazan, G. C.; Sperry, C. K. *J. Am. Chem. Soc*. **1997**, *119*, 9305. (g) Bazan, G. C.; Rodriguez, G.; Ashe, A. J., III; Al-Ahmad, S.; Kampf, J. W. *Organometallics* **1997**, *16*, 2492. (h) Bazan, G. C.; Rodriguez, G.; Ashe, A. J., III; Al-Ahamad, S.; Müller, C. *J. Am. Chem. Soc*. **1996**, *118*, 2291.

(3) (a) Bei, X.; Kreuder, C.; Swenson, D. C.; Jordan, R. F.; Young, V. G., Jr. *Organometallics* **1998**, *17*, 1085. (b) Yoshida, M.; Jordan, R. F. *Organometallics* **1997**, *16*, 4508. (c) Yoshida, M.; Crowther, D. J.; Jordan, R. F. *Organometallics* **1997**, *16*, 1349. (d) Crowther, D. J.; Swenson, D. C.; Jordan, R. F. *J. Am. Chem. Soc*. **1995**, *117*, 10403. (e) Bowen, D. E.; Jordan, R. F.; Rogers, R. D. *Organometallics* **1995**, *14*, 3630. (f) Kreuder, C.; Jordan, R. F.; Zhang, H. *Organometallics* **1995**, *14*, 2993. (g) Uhrhammer, R.; Su, Y.-X.; Swenson, D. C.; Jordan, R. F. *Inorg. Chem*. **1994**, *33*, 4398. (h) Bazan, G. C.; Schaefer, W. P.; Bercaw, J. E. *Organometallics* **1993**, *12*, 2126. (i) Uhrhammer, R.; Crowther, D. J.; Olson, J. D.; Swenson, D. C.; Jordan, R. F. *Organometallics* **1992**, *11*, 3098. (j) Crowther, D. J.; Baenziger, N. C.; Jordan, R. F. *J. Am. Chem. Soc*. **1991**, *113*, 1455.

(4) Kim, D.-H.; Won, J. H.; Kim, S.−J.; Ko, J.; Kim, S. H.; Cho, S.; Kang, S. O. *Organometallics* **2001**, *20*, 4298.

(5) Lee, Y.-J.; Lee, J.-D.; Jeong, H.-J.; Son, K.-C.; Ko, J.; Cheong, M.; Kang, S. O. *Organometallics* **2005**, *24*, 3008.

(6) Lee, Y.-J.; Lee, J.-D.; Ko, J.; Kim, S. H.; Kang, S. O. *Chem. Commun*. **2003**, 1364.

(7) Bazan, G. C.; Donnelly, S. J.; Rodriguez, G. *J. Am. Chem. Soc*. **1995**, *117*, 2671.

(8) (a) Rodriguez, G.; Bazan, G. C. *J. Am. Chem. Soc*. **1997**, *119*, 343. (b) Rodriguez, G.; Bazan, G. C. *J. Am. Chem. Soc*. **1995**, *117*, 10155.

(9) Pindado, G. J.; Thornton-Pett, M.; Bochmann, M. *J. Chem. Soc., Dalton Trans*. **1997**, 3115.

(10) (a) Plesek, J.; Hermanek, S.; Stibr, B. *Inorg. Synth*. **1983**, *22*, 231. (b) Wiesboeck, R. A.; Hawthorne, M. F. *J. Am. Chem. Soc*. **1964**, *86*, 1642.

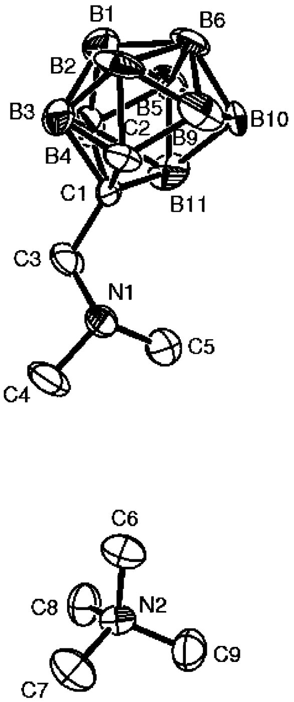

Figure 1. Molecular structure of **2a**·NC_4H_{12} with thermal ellipsoids drawn at the 30% level.

in the $^{11}B\{^1H\}$ NMR spectrum in the range −12 to −38 ppm and the presence of an absorption at ca. −3.0 ppm in the ^1H NMR spectrum imply a B−H−B interaction on the C_2B_3 open face. Most importantly, the ^1H NMR spectra of these complexes displayed a singlet pattern for the two methyl protons of the dimethylamino group at 2.70 (**3a**)/2.50 (**3b**) ppm. The methylene protons of the NCH_2 group are, however, diastereotopic, each giving rise to an AB spin pattern (2.92, 3.31 (**3a**)/2.72, 2.80 (**3b**) ppm). Further deprotonation of this bridge hydrogen with KH gave the corresponding dianionic ligand $[Dcab^N]^{2-}$, [*nido*-7-$NMe_2(CH_2)$-8-R-7,8-$C_2B_9H_9]^{2-}$.

Reaction of the Ligand with Group 4 Metal Complexes MX_4. Reaction of the dianionic compounds of **3** with $TiCl_4$ in toluene gave new types of CGC complexes, formulated as the aminodicarbollyl species $(Dcab^N)TiCl_2$ (**4**) (Scheme 1).

The precise structures of these compounds are unknown due to our inability to obtain single crystals for X-ray analysis. Complexes **4** decomposed slowly in solution or during crystallization. Several structural features were established from the spectral data yielded by **4**. The deprotonation of **3** was evident from the disappearance of the bridge hydrogen of B−H−B and N−H (^1H NMR: δ −3.01, 8.67 (**3a**) and −2.82, 8.33 (**3b**)). The ^1H NMR spectra of **4** revealed two signals for the methyl groups at the dimethylamino group of the side chain due to the asymmetric titanium metal center. The methylene protons of the NCH_2 groups in **4** were diastereotopic, each giving rise to an AB spin pattern. The most significant difference between the ^1H NMR spectra of **3** and **4** was the downfield shift of signals for the methylene proton of NCH_2. For complexes **2** these signals were observed at about 2.3 ppm, while **4** showed values of 2.72−3.31 ppm. The signals for the methyl protons at the dimethylamino group were also shifted downfield (from 1.68 to 2.11 ppm). Corresponding downfield shifts for the NCH_2 adjacent to the nitrogen atom were also observed in the ^{13}C NMR spectra. This observation is consistent with similar findings for other intramolecularly coordinated metal complexes that contain methylene spacers. Examples are complexes such as $(Dcab^N)ML_2$ (M = Ti, L = Cl;[11] M = Fe, Ru, L = Lewis base;[12] M = Ni, L = PPh_3[13]). In addition, the ^{11}B chemical shifts were similar to those observed for other dicarbollyl metal complexes and support the proposed η^5-coordination.[3,14] The spectroscopic data for complexes **4** indicated that the dimethylamino group of the side chain was coordinated to the metal center in all cases. Compounds **4** are among the first examples of dicarbollyl group 4 metal complexes with intramolecular coordination of a dimethylaminomethyl donor function in the side chain, although Hosmane and co-workers have independently reported the synthesis of C_2B_3-metallacarborane analogues and have discussed their reactivity.[14e,f] Also, Xie and co-workers recently described the synthesis and olefin polymerization activities of group 4 metal complexes containing imido/amino-tethered C_2B_3 dicarbollyl ligand systems.[15] The new dicarbollylamino complexes **4** were prepared from $TiCl_4$ and an equivalent amount of nucleophile **3** in toluene, as shown in Scheme 1. The pure products, which ranged from red to dark red in color, were isolated by recrystallization in toluene. Typically, the yields of **4** were on the order of 32−41%.

Scheme 2. Alternate Synthetic Route for the Formation of Group 4 Metal CGC Complexes[a]

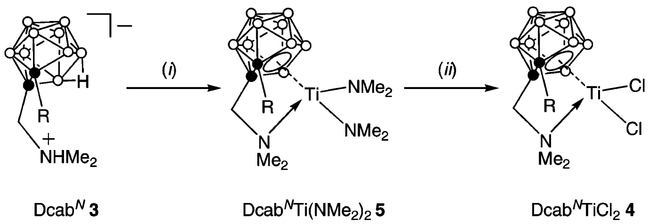

[a] Reagents and conditions: (*i*) $Ti(NMe_2)_4$, toluene, 25 °C; (*ii*) Me_3SiCl, CH_2Cl_2, 25 °C (R = H, **a**; Me, **b**).

Due to the low yield of the titanium complexes, we devised a direct metalation process using the zwitterionic aminomethyldicarbollide, $Dcab^NH$ (**3**). As shown in Scheme 2, reaction of **3** with $Ti(NMe_2)_4$ in toluene produced the desired mono(dicarbollide) complexes $(Dcab^N)Ti(NMe_2)_2$ (**5**) in good yields (86−88%). The corresponding chlorinated derivatives $Dcab^NTiCl_2$ (**4**) were prepared from the amido complexes **5** and a slight excess of Me_3SiCl in CH_2Cl_2 solution. This procedure gave the desired CGC-type derivative **4** in much higher yield than was achieved using the reaction described in Scheme 1. We believe that the metathesis reaction involving the dianionic compounds of **3** included a complex redox reaction with $TiCl_4$.

In contrast to the above reactions, where two amine ligands are eliminated from $Ti(NMe_2)_4$ in the presence of the multidentate ligand $DcabH_2^N$ (**3**), treatment of $Zr(NMe_2)_4$ with **3** gave the untethered complexes $(Dcab^N)Zr(NMe_2)_2(HNMe_2)$ (**6**) in good yields (77−82%). The detachment of the side arm during the reaction in Scheme 3 was evident from the change in the

---

(11) Wang, J.; Vyakaranam, K.; Maguire, J. A.; Quintana, W.; Teixidor, F.; Viòas, C.; Hosmane, N. S. *J. Organomet. Chem.* **2003**, *680*, 173.

(12) Park, J.-S.; Kim, D.-H.; Ko, J.; Kim, S. H.; Cho, S.; Lee, C.-H.; Kang, S. O. *Organometallics* **2001**, *20*, 4632.

(13) Park, J.-S.; Kim, D.-H.; Kim, S.-J.; Ko, J.; Kim, S. H.; Cho, S.; Lee, C.-H.; Kang, S. O. *Organometallics* **2001**, *20*, 4483.

(14) (a) Su, Y.-X.; Reck, C. E.; Guzei, I. A.; Jordan, R. F. *Organometallics* **2000**, *19*, 4858. (b) Houseknecht, K. L.; Stockman, K. E.; Sabat, M.; Finn, M. G.; Grimes, R. N. *J. Am. Chem. Soc.* **1995**, *117*, 1163. (c) Oki, A. R.; Zhang, H.; Hosmane, N. S. *Organometallics* **1991**, *10*, 3964. (d) Manning, M. J.; Knobler, C. B.; Khatter, R.; Hawthorne, M. F. *Inorg. Chem.* **1991**, *30*, 2009. (e) Siriwardane, U.; Zhang, H.; Hosmane, N. S. *J. Am. Chem. Soc.* **1990**, *112*, 9637. (f) Zhu, Y.; Vyakaranam, K.; Maguire, J. A.; Quintana, W.; Teixidor, F.; Viñas, C.; Hosmane, N. S. *Inorg. Chem. Commun.* **2001**, *4*, 486.

(15) Gao, M.; Tang, Y.; Xie, M.; Qian C.; Xie, Z. *Organometallics* **2006**, *25*, 2578.

Scheme 3. Alternate Synthetic Route for the Formation of Group 4 Metal CGC Complexes[a]

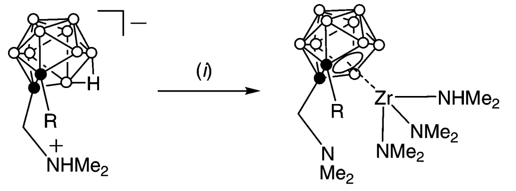

Dcab^N **3** Dcab^{N}Zr(NMe$_2$)$_2$(HNMe2) **6**

[a] Reagents and conditions: (*i*) Zr(NMe$_2$)$_4$, toluene, 25 °C (R = H, **a**; CH$_3$, **b**).

Scheme 4. Synthesis of Bis(aminomethyldicarbollyl) Group 4 Metal Complexes[a]

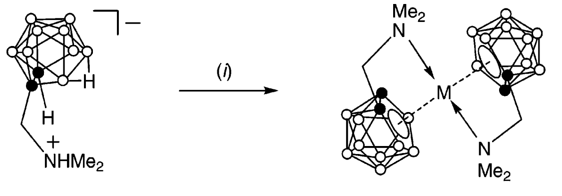

Dcab^N **3a** (Dcab^N)$_2$M (M = Ti, **7**; Zr, **8**; Hf, **9**)

[a] Reagents and conditions: (*i*) (*a*) KH, THF, 0 °C; (*b*) MCl$_4$, toluene, −78 °C (M = Ti, Zr, Hf).

Scheme 5. Isolation of Intramolecularly Stabilized Titanium Alkoxy Complexes[a]

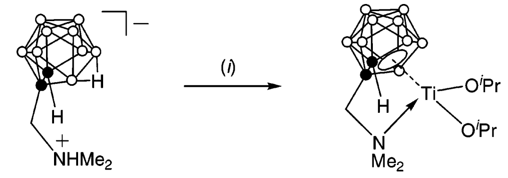

Dcab^N **3a** Dcab^{N}Ti(O^{i}Pr)$_2$ **10**

[a] Reagents and conditions: (*i*) Ti(O^{i}Pr)$_4$, toluene, 25 °C.

Scheme 6. Reactivity of Intramolecularly Stabilized Titanium Amido Complexes with Phenols[a]

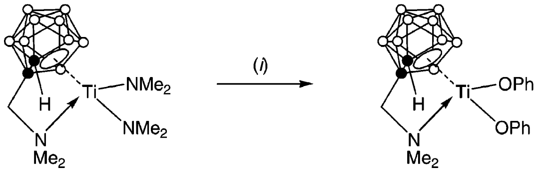

Dcab^{N}Ti(NMe$_2$)$_2$ **5** Dcab^{N}Ti(OPh)$_2$ (Ph = C$_6$H$_5$, **11**; 2-MeC$_6$H$_4$, **12**)

[a] Reagents and conditions: (*i*) PhOH, toluene, 80 °C (Ph = C$_6$H$_5$, 2-MeC$_6$H$_4$).

signal corresponding to the bridgehead methylene unit of the NC*H*$_2$ in the ^{1}H NMR spectrum from AB to a broad singlet pattern. Compounds **6a** and **6b** were readily identified from their spectroscopic properties (see Supporting Information). The dimethylamine HN*Me*$_2$ moieties of **6** were recognized from features in the ^{1}H NMR spectra at the characteristic positions of δ 2.69 (**6a**) and 2.55 (**6b**).

At the outset of these studies we expected to synthesize the dichloro-zirconium and dichloro-hafnium complexes via a route analogous to that described for the corresponding titanium complex **4**. However, reaction of the dianion of **3a** with MCl$_4$ (M = Zr, Hf) in toluene resulted in (Dcab^N)$_2$M (M = Zr, **8**; Hf, **9**) (Scheme 4). The first evidence for the formation of the 1:2 complexes **8** and **9** came from ^{1}H NMR spectra. In contrast to the 1:1 complex **4a**, the methylene protons of the NC*H*$_2$ in **8** and **9** showed different chemical shifts at around δ 2.68−2.89 (doublet, J_{H-H} = 14 Hz) in benzene-d_6 solution at room temperature. Similarly, the reaction of TiCl$_4$ with 2 equiv of the dianionic form of **3a** in toluene gave complex (Dcab^N)$_2$Ti (**7**) (Scheme 4).

Complexes (Dcab^N)$_2$M (**7**−**9**) are very air- and moisture-sensitive, show good solubility in aromatic solvents, but are poorly soluble in aliphatic hydrocarbons. These complexes were completely characterized by elemental analysis and NMR spectroscopy. Consistent with the proposed structure, the ^{1}H NMR spectra of (Dcab^N)$_2$M (**7**−**9**) at room temperature showed two signals for the methyl protons of the dimethylamino groups and two signals for the C−H moieties on the dicarbollyl groups. The two protons in each of the methylene NC*H*$_2$ links are diastereotopic and gave rise to an AB coupling pattern.

The reaction of the ligand **3a** with 1 equiv of Ti(O^{i}Pr)$_4$ in toluene yielded the alkoxide-stabilized CGC-type complexes (Dcab^N)Ti(O^{i}Pr)$_2$ (**10**) (Scheme 5). As was seen in the amine-elimination reactions of Scheme 2, two O^{i}Pr ligands were easily eliminated from Ti(O^{i}Pr)$_4$ in the presence of the multidentate ligand DcabH$_2{}^N$ (**3a**). The signals for the methyl protons of the dimethylamino group and the methylene protons of the NC*H*$_2$ in **10** were shifted upfield compared to signals from the Ti-NMe$_2$ complexes **5a**. The Ti-O^{i}Pr ^{1}H NMR resonance was at δ 1.24 and 1.26 for [−CH*Me*$_2$] and δ 4.49 for [−C*H*Me$_2$].

The reaction of (Dcab^N)Ti(NMe$_2$)$_2$ (**5a**) with 2 equiv of phenol derivatives in toluene gave complexes **11** and **12**. In fact, when **5a** reacted with less hindered phenols such as phenol and 2-methylphenol, the expected aryloxy substitution was observed to generate the corresponding bis-aryloxy-stabilized complexes (Dcab^N)Ti(OPh)$_2$ (Ph = C$_6$H$_5$, **11**; 2-Me-C$_6$H$_4$, **12**) in high yield (Scheme 6). Both the phenoxy-substituted **11** and 2-methylphenoxy-substituted **12** complexes yielded ^{1}H NMR signals very similar to those of the alkoxy complex **10**. The signals from the methyl proton of the dimethylamino group and the methylene protons of the NC*H*$_2$ in **11** and **12** were shifted upfield in comparison to signals from the starting material **5a**. The (Dcab^N)Ti(OPh)$_2$ complex **11** showed two Ti-O*Ph* ^{1}H NMR signals at δ 6.90−7.37, and the ^{1}H NMR resonance of the methyl proton of the Ti-O(2-*Me*Ph) **12** was observed at δ 2.72 and 2.74.

X-ray Crystal Structure Analyses. X-ray structural determinations confirmed the expected constrained geometry structures illustrated in Figures 2−7. Six of the (Dcab^N)M(IV) (M = Ti, Zr) complexes prepared in the course of this study were characterized by X-ray diffraction. These included mono-chelated (**5a** and **5b**) and bis-chelated (**8**) complexes and the corresponding aryloxy-substituted mono-chelated complexes (**11** and **12**). Some general structural features are compared in Table 3, where selected data on the Dow-CGC systems are also presented. Detailed information on structural determinations and the structural features of all six compounds discussed here are provided in the Supporting Information.

Important evidence supporting the intramolecular coordination of the dimethylamino group to the titanium metal in complex **5** is provided by X-ray crystal structure analysis. As shown in Figure 2, complex **5a** possesses a crystallographic disorder imposed by mirror symmetry. Thus, cage atoms Ti(1), C(1), B(1), and B(4), and the N(1) and C(3) of the dimethylamino group, lie on the crystallographic mirror plane. As a consequence, the untethered carboranyl carbon atom C(2) is disor-

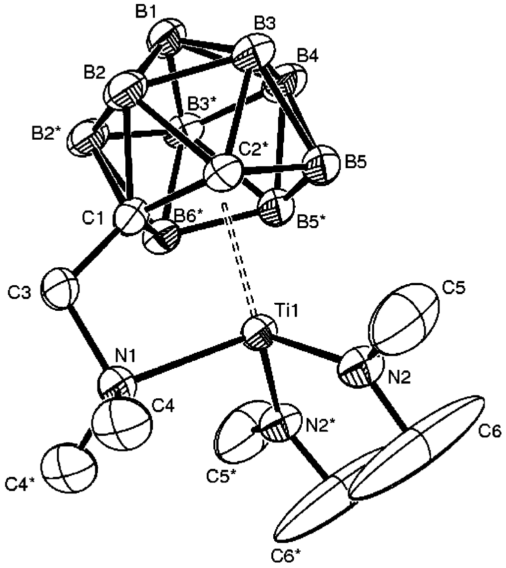

Figure 2. Molecular structure of **5a** with thermal ellipsoids drawn at the 30% level.

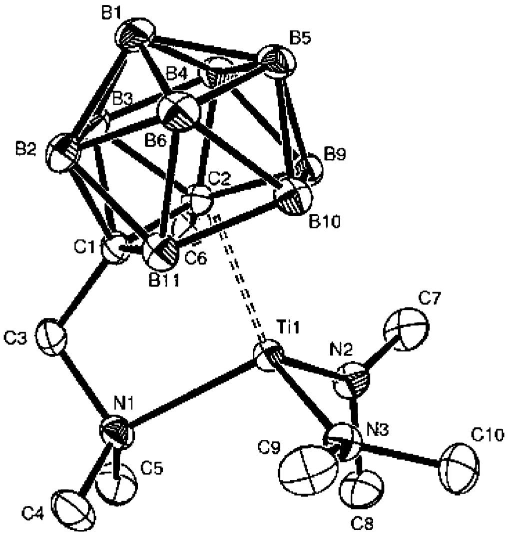

Figure 3. Molecular structure of **5b** with thermal ellipsoids drawn at the 30% level.

dered with respect to this plane so that the atomic positions designated by C(2*) and B(6*) are 50% occupied by C and 50% occupied by B. The molecule is a $Ti(NMe_2)_2$ unit that is bonded to a pentahapto dicarbollyl ligand. The dimethylamino fragment coordinates to the titanium in the remaining basal site of the overall three-legged "piano-stool" conformation, giving a five-membered ring. The titanium metal is centered approximately over the ring, giving rise to a Ti(1)−C_2B_3 face (centroid) distance of 1.931 Å. Selected bond lengths and angles for **5a** are listed in Table 3 and in the Supporting Information. The Ti(1)−N(1) bond length is 2.220(7) Å, a value that lies within the usual range for a dative bond between titanium and nitrogen atoms.[16,17]

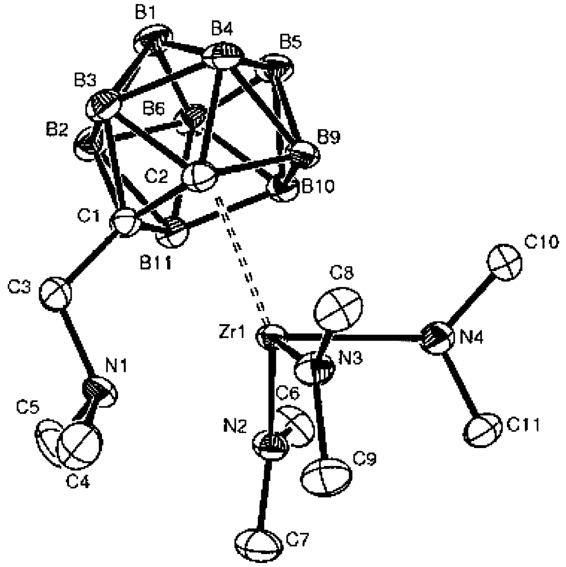

Figure 4. Molecular structure of **6a** with thermal ellipsoids drawn at the 30% level.

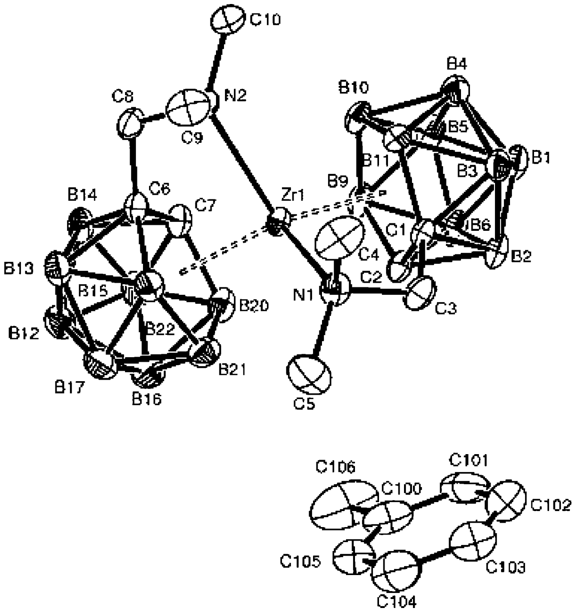

Figure 5. Molecular structure of **8**·C_7H_8 with thermal ellipsoids drawn at the 30% level.

As shown in Figure 3, complex **5b** serves as an example to outline the general characteristics of this new class of compounds. The central titanium atom in **5b** is pseudotetrahedrally coordinated to a pair of dimethylamido ligands (Ti(1)−N(2)/(N3) 1.900(2)/1.901(2) Å), the NMe_2 side arm, and the C_2B_3 plane of the dicarbollyl ligand. Observation of a Ti(1)−N(1) distance of 2.255(2) Å, which is consistent with a Ti−N(sp^3) single bond (2.225(2) Å),[17] confirms that the N-donor atom is coordinated to the metal in a strain-free manner. The C_2B_3 ligand is η^5-coordinated to titanium, but rather unsymmetrically, probably because of the strain imposed on the system by the short C(1) bridge. The Ti(1)−C(1) (2.385(2) Å) linkage is markedly shorter than the Ti(1)−C(2) (2.484(2) Å) linkage. The Ti(1)−B(11) (2.359(3) Å) linkage of **5b** is, however, shorter than the Ti(1)−C(1) linkage, and these linkages are in turn shorter than the Ti(1)−B(9)/B(10) (2.456(3)/2.426(3) Å) linkage. The corresponding C_2B_3(centroid)−C(1)−C(3) angle is 146.99°. The endocyclic C(1)−C(3)−N(1) bond angle is 106.57(19)°, which deviates from the tetrahedral sp^3-C value. The "constrained geometry" character in a series of related compounds is probably best characterized by the C_2B_3(centroid)−metal−

---

(16) (a) Kotov, V. V.; Avtomonov, E. V.; Sundermeyer, J.; Harms, K.; Lemenovskii, D. A. *Eur. J. Inorg. Chem.* **2002**, 678. (b) Cheung, M.-S.; Chan, H.-S.; Xie, Z. *Organometallics* **2005**, *24*, 3037. (c) Cheung, M.-S.; Chan, H.-S.; Bi, S.; Lin, Z.; Xie, Z. *Organometallics* **2005**, *24*, 4333.

(17) Kwong, W.-C.; Chan, H.-S.; Tang, Y.; Xie, Z. *Organometallics* **2004**, *23*, 4301.

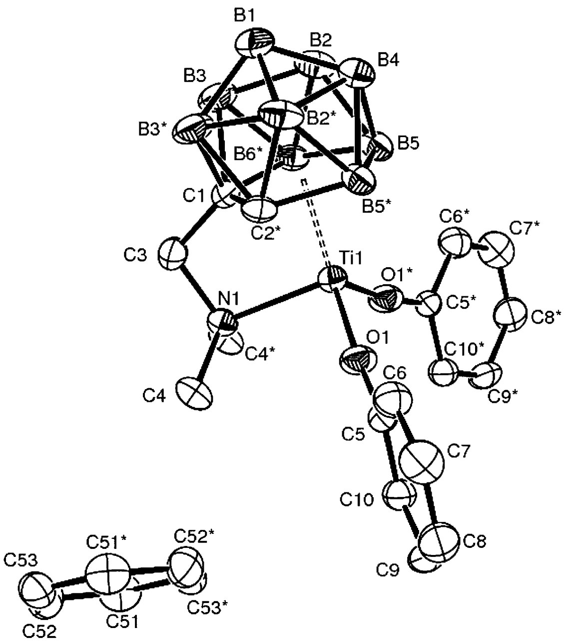

Figure 6. Molecular structure of **11**·C_6H_6 with thermal ellipsoids drawn at the 30% level.

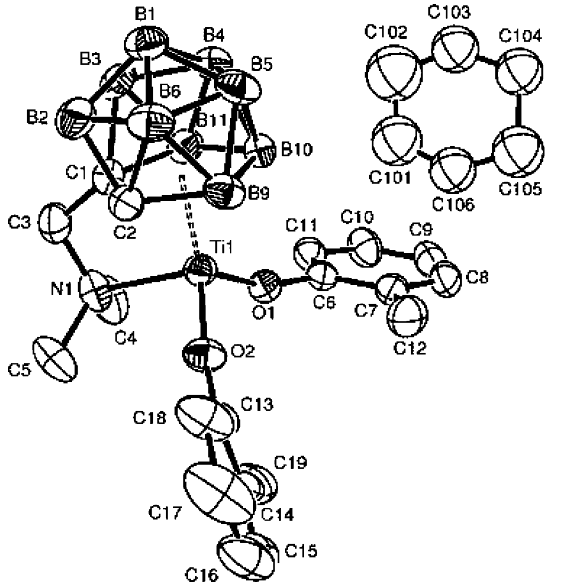

Figure 7. Molecular structure of **12**·C_6H_6 with thermal ellipsoids drawn at the 30% level.

nitrogen angle, which responds sensitively to steric and electronic geometry changes. In **5b**, this angle is 98.22°.

The X-ray crystal structure of **6a** (Figure 4) revealed that the Zr atom essentially adopts a half-metallocene-type geometry, having an η^5-bonding mode with the dicarbollyl ligand and an η^1-bonding mode with the two dimethylamido ligands and with the dimethylamine ligand. In particular, structural studies revealed that the dimethylamine freed from $Zr(NMe_2)_4$ was recoordinated to the zirconium atom of **6a** in one of the leg positions of the piano-stool geometry. The formation of **6a** presumably results from attachment of a liberated amine ligand and concomitant detachment of a dimethylamine unit of the side arm by a ligand substitution reaction. In **6a**, the Zr(1)−N(2)/N(3) distance is 2.054(2)/2.033(2) Å and the Zr(1)−N(4) distance is 2.450(2) Å. These values correlate well with those found in similar complexes (η^5-$C_2B_9H_{11}$)$Zr(NEt_2)_2(HNEt_2)$,[3e] which have values of 2.047(3)/2.029(3) Å for the Zr−amido distance and 2.360(3) Å for the Zr−amino distance, respectively. As expected, the Zr−amino distance is much longer than the Zr−amido distance[3e,18−21] and N(4) adopts a pyramidal geometry.

The X-ray crystal structure of **8** (Figure 5) revealed that the Zr atom essentially adopts an η^5-bonding posture with the dicarbollyl rings and an η^1-bonding posture with the dimethylamino side groups. Overall, **8** adopts the distorted-tetrahedral coordination geometry of [Zr(Dcab^N)$_2$], with 2-fold rotational symmetry. The Zr(1)−N(1) distance of 2.46−2.49 Å confirms that the N-donor atom is coordinated to the metal in a strain-free manner and the bond distance is consistent with a Zr−N(sp^3) single bond.[3e,21] The noticeable shortening, compared to **6a**, of the Zr(1)−C_2B_3(centroid) distance (2.079 Å) [where C_2B_3(centroid) is the centroid of the dicarbollyl ring] and the expansion of the C_2B_3(centroid)−Zr(1)−C_2B_3(centroid) (138.05°) and N(1)−Zr(1)−N(2) (103.40(1)°) angles in **8** can be explained by the chelating effect introduced by the aminomethyldicarbollyl ligand. The preferred formation of a bis(dicarbollyl) over a mono(dicarbollyl) complex can be ascribed to the greater ionic radii of zirconium and hafnium compared to that of titanium.[3a,f,22]

The molecular structure of **11**, determined by X-ray diffraction, is shown in Figure 6. The structure has a strong resemblance to that of **5a**. As expected, complex **11** possesses a crystallographic disorder imposed by mirror symmetry. Cage atoms Ti(1), C(1), B(1), and B(4), and the aminomethyl atoms N(1) and C(3), lie on the crystallographic mirror plane. As a consequence, the untethered carboranyl carbon atom is disordered with respect to this plane such that the atomic positions designated by C(2*) and B(6*) are 50% occupied by C and 50% occupied by B. Structural analysis of **11** showed that the dimethylamino group was intramolecularly coordinated to the titanium atom. Therefore, the complex adopts an essentially "piano-stool" structure with the titanium atom η^5-coordinated on one side by a dicarbollyl group and the other by the dimethylamino group and two phenoxy ligands. The C_2B_3(centroid)−Ti(1) bond length in **11** is 1.881 Å. The Ti(1)−N(1) bonds are shorter (2.177(3) Å) than those in the (Dcab^N)Ti(NMe$_2$)$_2$ analogues **5a** (2.220 (7) Å).

The geometry and the metric parameters of complex **12** (Figure 7) are similar to those of the related complex **11**. However, atoms C(8), C(9), C(10), and C(11) in the phenol ring are disordered over two positions. Therefore, the site-occupancies were refined by using PART instruction in SHELXL-97, and finally they reached 0.28(2) and 0.72(2), respectively. The C_2B_3(centroid)−Ti(1) bond length in **12** is 1.870 Å. The Ti(1)−N(1) bonds are shorter (2.190(4) Å) in **12** compared to those in the (Dcab^N)Ti(NMe$_2$)$_2$ analogues **5a**. The Ti(1)−O(1)/O(2) bond lengths 1.782(3)/1.783(4) are shorter than the typical range found in other aryloxo complexes of the type $CpTiX_3$ (1.790(18)−1.828(1) Å).[23] Again, the C(1)−C(3) vector is oriented out of the C_2B_3 plane. The C(1)−C(3)−N(1) angle is 105.2(4)°, and the C_2B_3(centroid)−Ti(1)−N(1) angle is 99.85°.

Olefin Polymerization Experiments. Preliminary investigations were carried out to study the behavior of the (Dcab^N)TiCl$_2$ and (Dcab^N)Ti(OR)$_2$ (R = ^{i}Pr, C_6H_5, 2-Me-C_6H_4) catalyst

---

(18) Zi, G.; Li, H.-W.; Xie, Z. *Organometallics* **2002**, *21*, 3850.

(19) Wang, H.; Wang, Y.; Li, H.-W.; Xie, Z. *Organometallics* **2001**, *20*, 5110.

(20) (a) Wang, Y.; Wang, H.; Li, H.-W.; Xie, Z. *Organometallics* **2002**, *21*, 3311. (b) Xie, Z. *Acc. Chem. Res.* **2003**, *36*, 1. (c) Lee, M. H.; Hwang, J.-W.; Kim, Y.; Han, Y.; Do, Y. *Organometallics* **2000**, *19*, 5514.

(21) Carpenetti, D. W.; Kloppenburg, L.; Kupec, J. T.; Petersen, J. L. *Organometallics* **1996**, *15*, 1572.

(22) Shannon, R. D. *Acta Crystallogr.* **1976**, *A32*, 751.

Table 1. Comparison of the NMR Spectroscopic Data for Compounds 2a, 3a, 3b, 4a, 4b, 5a, 5b, 6a, 6b, 7, 8, 9, 10, 11, and 12

compound	$^{1}H_{CH2}$	$^{1}H_{N(CH3)2}$	$^{1}H_{M-N(CH3)2}$	$^{13}C_{CH2}$	$^{13}C_{N(CH3)2}$	$^{13}C_{M-N(CH3)2}$
2a[a]	2.38, 2.43	2.11		69.57	45.74	
3a[a]	2.92, 3.31	2.70		54.96	43.48, 44.63	
3b[a]	2.72, 2.80	2.50		57.53	43.01, 47.79	
4a[c]	2.70, 3.43	1.68, 1.74		69.76	54.36, 58.63	
4b[c]	3.20, 3.36	2.09, 2.11		69.85	53.25, 57.86	
5a[b]	2.81, 3.59	2.34, 2.42	3.57, 3.61	57.89	46.91, 48.67	49.73, 51.52
5b[b]	2.78, 3.71	2.50, 2.85	3.51, 3.63	59.63	47.66, 49.01	50.66, 52.39
6a[b]	3.20, 3.45	2.71, 2.85	3.24, 3.36	60.03	42.53, 44.27	49.27, 50.50
6b[b]	3.43, 3.55	2.54, 2.73	3.14, 3.26	58.57	39.82, 41.61	45.18, 46.38
7[c]	2.70, 3.02	1.39, 1.75		72.88	55.04, 56.33	
8[c]	2.74, 2.89	1.81, 2.07		72.99	52.65, 56.01	
9[c]	2.68, 2.89	1.79, 2.19		74.10	54.86, 57.07	
10[b]	3.05, 3.15	1.35		49.50, 52.90	27.15	
11[c]	2.87, 3.10	1.62, 1.89		55.82, 62.55	21.27, 21.60	
12[c]	3.61, 3.73	2.05, 2.18		56.45, 60.57	37.50, 40.95	

[a] $(CD_3)_2SO$ was used as the solvent, and the chemical shifts are reported relative to the residual H of the solvent. [b] $CDCl_3$ was used as the solvent, and the chemical shifts are reported relative to the residual H of the solvent. [c] $C_6D_6$was used as the solvent, and the chemical shifts are reported relative to the residual H of the solvent.

Table 2. Ethylene Polymerization Examples Employing 4a, 4b, 10, 11, and 12[a]

entry	catalyst	cocatalyst	scavenger	initiation temp (°C)	activity[b]	$M_w \times 10^{-4}$ [c]	M_w/M_n [c]
1	**4a**	$Ph_3CB(C_6F_5)_4$	mMAO	60	2.9	0.8	3.0
2	**4b**	$Ph_3CB(C_6F_5)_4$	mMAO	60	2.4	0.6	2.6
3	**10**	$Ph_3CB(C_6F_5)_4$	mMAO	60	1.4	0.3	3.3
4	**11**	$Ph_3CB(C_6F_5)_4$	mMAO	60	0.3	0.1	3.2
5	**12**	$Ph_3CB(C_6F_5)_4$	mMAO	60	0.3	0.1	2.9
6	Dow-CGC (**A**)	$Ph_3CB(C_6F_5)_4$	mMAO	60	26.0	36.7	3.6

[a] Polymerization condition: semibatch type 500 mL autoclave reactor, solvent = cyclohexane, ethylene pressure = 30 kg/cm^2, total solution volume = 300 mL, catalyst concentration = 3.3 μM, [catalyst]:[cocatalyst]:[scavenger] = 1:1.5:100, reaction time = 10 min. [b] $\times 10^3$ kg of polymer/(mol of Ti·h). [c] Weight average molecular weight (g/mol) and molecular weight distribution measured by PL210 GPC at 135 °C.

Table 3. Characteristic Structural Parameters of 5a, 5b, 6a, 8·C$_7$H$_8$, 11·C$_6$H$_6$, and 12·C$_6$H$_6$

	5a	**5b**	**6a**	**8·C$_7$H$_8$**	**11**·C$_6$H$_6$	**12**·C$_6$H$_6$	**CGC**[c]
M−C1	2.349(7)	2.385(2)	2.617(2)	2.467(3), 2.469(3)	2.332(3)	2.327(5)	
M−C2	2.386(7)	2.359(3)	2.655(3)	2.473(4), 2.497(4)	2.353(3)	2.343(6)	
M−B9	2.434(8)	2.426(3)	2.609(3)	2.573(5), 2.592(5)	2.388(3)	2.362(6)	
M−B10	2.434(8)	2.456(3)	2.577(3)	2.593(5), 2.580(4)	2.388(3)	2.395(6)	
M−B11	2.386(7)	2.484(2)	2.567(3)	2.504(3), 2.489(4)	2.353(3)	2.344(6)	
M−DCab$_{(centr)}$	1.931	1.950	2.180	2.077, 2.081	1.881	1.870	2.030
M−N1	2.220(7)	2.255(2)	2.579(2)	2.488(3), 2.460(3)	2.178(3)	2.190(4)	1.907(3)
M−N2	1.893(5)	1.900(2)	2.054(2)				2.264(1)
M−N3	1.893(5)	1.901(2)	2.033(2)				2.264(1)
M−N4			2.450(2)				
DCab$_{(centr)}$−C1−C3	147.27	146.99	151.02	151.37, 151.95	146.23	146.03	
N1−M−DCab$_{(centr)}$	99.39	98.22	86.85	93.47, 93.43	99.97	99.85	107.6
C1−C3−N1	106.9(7)	106.57(19)	109.9(2)	108.3(3), 108.1(3)	104.9(3)	105.2(4)	
N2−M−N3	102.5(3)	99.77(9)	116.39(9)				102.97(7)
M−O1					1.779(2)	1.782(3)	
M−O2					1.779(2)	1.783(4)	
O1−M−O2					102.4(1)	103.3(2)	

[a] Bond lengths in Å, angles in deg. [b] Value from two independent molecules in the unit cell. [c] $(C_5Me_4)-(C_2H_6)Si-NBu^tTiCl_2$.

systems in olefin polymerization. Some representative data from ethylene polymerization reactions are listed in Table 3. The data show that most of the (Dcab^N)TiX$_2$ systems exhibited rather low activities as ethylene polymerization catalysts under the chosen experimental conditions (when activated with excess $[Ph_3C][B(C_6F_5)_4]$ in cyclohexane at 60 °C and with 30 atm of ethylene). The activities of **4**/$[Ph_3C][B(C_6F_5)_4]$ catalysts were highest (entries 1 and 2 in Table 3), but even these systems were much less active than the Dow-CGC-type catalyst **A**/$[Ph_3C][B(C_6F_5)_4]$ (Table 3, entry 6). The introduction of a methyl group at the 2-position of the dicarbollyl ligand resulted in no significant improvement in catalytic performance and, indeed, somewhat lowered polymerization activity. The product molecular weight distributions obtained from complexes **4** were 2.6 and 3.0, respectively (Table 3). We also investigated the efficacy with which the bis-aryloxy titanium(IV) complexes **10**−**12** catalyzed ethylene polymerizations. The polymerization of ethylene at 60 °C in the presence of catalytic precursors **10**−**12** with $[Ph_3C][B(C_6F_5)_4]$ as a cocatalyst and mMAO-7 as a scavenger was investigated. As shown in Table 3, these complexes showed very low catalytic performance in the polymerization of ethylene. The present results thus show that the dicarbollylamino-chelated CGC-type group 4 metal complexes have very low catalytic activities in polymerization of olefins.

---

(23) (a) Nomura, K.; Naga, N.; Miki, M.; Yanagi, K.; Imai, A. *Organometallics* **1998**, *17*, 2152. (b) Firth, A. V.; Stewart, J. C.; Hoskin, A. J.; Stephan, D. W. *J. Organomet. Chem.* **1999**, *591*, 185. (c) Sturla, S. J.; Buchwald, S. L. *Organometallics* **2002**, *21*, 739. (d) Fenwick, A. E.; Phomphrai, K.; Thorn, M. G.; Vilardo, J. S.; Trefun, C. A.; Hanna, B.; Fanwick, P. E.; Rothwell, I. P. *Organometallics* **2004**, *23*, 2146. (e) Esteruelas, M. A.; López, A. M.; Mateo, A. C.; Oñate, E. *Organometallics* **2006**, *25*, 1448.

Conclusion

In summary, we prepared new types of mono-dicarbollylamino and bis-dicarbollylamino group 4 metal complexes. These complexes were fully characterized by NMR (^{1}H, ^{11}B, ^{13}C) and X-ray crystallography. Structural analyses of the complexes showed that the dimethylamino group was intramolecularly coordinated to the titanium atom. All complexes therefore had a "constrained-geometry" structure. With intramolecular coordination by a dicarbollylamino ligand at the titanium metal center, complex **5** was found to undergo ligand substitution toward nucleophiles such as chloride and alkoxide. In addition, we studied the use of these complexes as catalysts for ethylene polymerization. Unfortunately, in contrast to the DOW CGC catalyst, the titanium complexes **4**, **10**, **11**, and **12** showed low ethylene polymerization activities in the presence of $[Ph_3C][B(C_6F_5)_4]$. The derivatization of dicarbollyl ligands for the synthesis of new types of organometallic complexes is under active investigation.

Experimental Section

General Procedures. All manipulations were performed under a dry, oxygen-free nitrogen or argon atmosphere using standard Schlenk techniques or in a Vacuum Atmosphere HE-493 drybox. Toluene, hexane, and pentane were distilled under nitrogen from sodium/benzophenone. Dichloromethane was dried with CaH_2. Benzene-d_6 was distilled under nitrogen from sodium and stored in a Schlenk storage flask until needed. $CDCl_3$ was predried under CaH_2 and vacuum-transferred. *n*-BuLi (2.5 M in hexanes), KH, MCl_4 (M = Ti, Zr, Hf), and $Ti(O^iPr)_4$ were used as received from Aldrich and Strem Chemical. *o*-Carborane was purchased from KatChem and used after sublimation. The starting materials $M(NMe_2)_4$ (M = Ti, Zr) were either purchased from Strem Chemical or prepared by literature methods.[24] All ^{1}H (300.1 MHz, measured in $CDCl_3$), ^{11}B (96.3 MHz, measured in $CDCl_3$), and ^{13}C (75.4 MHz, measured in $CDCl_3$) NMR spectra were recorded on a Varian Mercury-300BB spectrometer unless otherwise stated. ^{1}H and ^{13}C NMR chemical shifts were measured relative to internal residual peaks from the lock solvent (99.5% $(CD_3)_2SO$, 99.9% $CDCl_3$, 99.5% C_6D_6) and then referenced to Me_4Si (0.00 ppm). All ^{11}B NMR chemical shifts were referenced to $BF_3{\cdot}O(C_2H_5)_2$ (0.0 ppm) with a negative sign, indicating an upfield shift. Elemental analyses were performed with a Carlo Erba Instruments CHNS-O EA1108 analyzer. All melting points were uncorrected. High-resolution mass spectra were measured at the Korea Basic Science Institute.

Preparation of $[NMe_4][$*nido*$\text{-}7\text{-}NMe_2CH_2\text{-}7,8\text{-}C_2B_9H_{10}]$, 2a. Compound **1a** (0.60 g, 3.0 mmol) was dissolved in degassed EtOH (20 mL), KOH (0.22 g, 4.0 mmol) was added, and the reaction mixture was heated to reflux for 12 h. CO_2 was bubbled through the cooled solution, and the resulting precipitate of K_2CO_3 was filtered off to afford a clear yellow solution. The ethanol was removed *in vacuo*, and the residue dissolved in H_2O (40 mL). An aqueous solution of NMe_4Cl (0.35 g, 3.2 mmol) was then added, resulting in the formation of a sticky white precipitate. The solution was extracted three times with acetone (3 × 30 mL), and the combined extract dried over anhydrous $MgSO_4$ to afford 0.74 g (2.8 mmol, 93%) of $NMe_4^+[$*nido*$\text{-}7\text{-}NMe_2CH_2\text{-}7,8\text{-}C_2B_9H_{11}]^-$ (**2a**). Recrystallization from an acetone/THF mixture gave a colorless crystalline solid. Mp: 130−133 °C (dec). Anal. Calcd for $C_9B_9H_{31}N_2$: C, 40.85; H, 11.81; N, 10.59. Found: C, 40.89; H, 11.92; N, 10.54. ^{11}B NMR (96.3 MHz, DMSO-d_6): δ −9.65 (1B), −10.32 (1B), −13.54 (1B), −16.71 (1B), −17.70 (1B), −19.32 (1B), −22.31 (1B), −33.12 (1B), −36.66 (1B). IR spectrum (KBr pellet, cm^{-1}): ν(B−H) 2537, ν(C−H) 3033.

Preparation of $[$*nido*$\text{-}7\text{-}HNMe_2CH_2\text{-}7,8\text{-}RC_2B_9H_{11}]$, 3a. Compound **1a** (0.6 g, 3.0 mmol) and KOH (0.22 g, 4.0 mmol) were dissolved in degassed EtOH (20 mL) and then refluxed under N_2 for 12 h. EtOH was removed under reduced pressure, and the residue was suspended in benzene (60 mL). Azeotropic distillation was then performed to remove H_2O and EtOH, and the remaining white solid was dried under vacuum overnight. The solid was mixed with benzene (30 mL) under N_2 to form a slurry, and then H_3PO_4 was added; the resulting two-phase mixture was stirred vigorously for 15 h. The volatiles were removed by rotary evaporation under reduced pressure, and the residue was washed with H_2O to yield an off-white solid. The product was purified by recrystallization from acetone to yield **3a** (0.50 g, 2.6 mmol) as a colorless crystalline solid in 87% yield. Mp: 143−145 °C (dec). Anal. Calcd for $C_5B_9H_{20}N$: C, 31.36; H, 10.53; N, 7.31. Found: C, 31.46; H, 10.50; N, 7.29. ^{11}B NMR (96.3 MHz, DMSO-d_6): δ −12.52 (2B), −15.40 (2B), −21.47 (3B), −33.99 (1B), −38.23 (1B). IR spectrum (KBr pellet, cm^{-1}): ν(B−H) 2492, 2540, ν(C−H) 2901, 2991, 3032, ν(N−H) 3167.

3b: Yield: 90% (0.55 g, 2.7 mmol). Mp: 146−149 °C (dec). Anal. Calcd for $C_6B_9H_{22}N$: C, 35.06; H, 10.79; N, 6.81. Found: C, 34.94; H, 10.75; N, 6.79. ^{11}B NMR (96.3 MHz, DMSO-d_6): δ −11.54 (3B), −16.29 (2B), −20.90 (2B), −34.85 (1B), −37.85 (1B). IR spectrum (KBr pellet, cm^{-1}): ν(B−H) 2461, 2509, 2542, ν(C−H) 2876, 2937, 2964, 3032, ν(N−H) 3186.

Preparation of $(Dcab^N)TiCl_2$ (R = H, a; CH_3, b), 4a. To a stirred 20 mL of THF solution containing **3a** (0.57 g, 3.0 mmol) was added slowly KH (0.29 g, 7.2 mmol) by side arm at 0 °C. The mixture was stirred for 3 h at room temperature, and the resulting clear yellow supernatant was decanted via syringe. Removal of the solvent *in vacuo* and washing with light petroleum afforded a yellow powder of the dianion of **3a** (0.51 g, 2.7 mmol, 90%). The dianion of **3a** (0.38 g, 2.0 mmol) was slurried in toluene and cooled to −78 °C, after which $TiCl_4$ (0.38 g, 2.0 mmol) was slowly added. The mixture was then warmed slowly to room temperature and stirred for 2 h. The formation of **4a** was demonstrated by ^{1}H NMR spectroscopy. Removal of the volatiles under vacuum provided the final crude product. Extraction of the residue with toluene (20 mL) followed by concentration to approximately half its volume and cooling to −10 °C resulted in crystallization of pure **4a** (0.20 g, 0.65 mmol, 32% yield). Anal. Calcd for $C_5B_9H_{18}N_1Ti_1Cl_2$: C, 19.48; H, 5.89; N, 4.54. Found: C, 19.33; H, 5.75; N, 4.36. ^{11}B NMR (96.3 MHz, $CDCl_3$): δ −9.63 (1B), −3.34 (1B), −1.63 (1B), 0.83 (1B), 2.63 (1B), 4.78 (1B), 6.39 (1B), 8.32 (1B), 26.33 (1B). IR spectrum (KBr pellet, cm^{-1}): ν(B−H) 2532, ν(C−H) 2876, 2910, 2974.

4b: A procedure analogous to that used to prepare **4a** was used, but starting from the dianion of **3b** (0.41 g, 2.0 mmol) in THF. Yield: 41% (0.26 g, 0.81 mmol). Anal. Calcd for $C_6B_9H_{20}N_1Ti_1Cl_2$: C, 22.36; H, 6.25; N, 4.35. Found: C, 22.22; H, 6.25; N, 4.35. ^{11}B NMR (96.3 MHz, $CDCl_3$): δ −8.43 (1B), −2.37 (1B), −0.67 (1B), 1.93 (1B), 4.44 (1B), 7.89 (1B), 10.17 (1B), 11.22 (1B), 28.14 (1B). IR spectrum (KBr pellet, cm^{-1}): ν(B−H) 2532, ν(C−H) 2872, 2930, 2960.

Preparation of $(Dcab^N)Ti(NMe_2)_2$ (R = H, a; CH_3, b), 5a. A representative procedure is as follows: over a period of 30 min, a 20 mL toluene solution of $Ti(NMe_2)_4$ (0.22 g, 1 mmol) was added to a stirred solution of **3a** (0.19 g, 1 mmol) in toluene (20 mL) at 0 °C. After addition was complete, the solution was removed from the cold bath and then stirred at room temperature for 1 h. The solvent was then removed under vacuum and the residue purified by recrystallization with a CH_2Cl_2/toluene mixture at −35 °C. **5a**: Yield: 86% (0.28 g, 0.86 mmol). Anal. Calcd for $C_9B_9H_{30}N_3Ti_1$: C, 33.21; H, 9.29; N, 12.91. Found: C, 32.95; H, 9.16; N, 12.69. ^{11}B NMR (96.3 MHz, $CDCl_3$): δ −25.19 (1B), −18.57 (2B),

---

(24) Diamond, G. M.; Jordan, R. F.; Peterson, J. L. *J. Am. Chem. Soc.* **1996**, *118*, 8024.

−13.97 (1B), −9.19 (2B), −3.89 (1B), 1.71 (1B), 12.13 (1B). IR spectrum (KBr pellet, cm^{-1}): ν(B−H) 2532, ν(C−H) 2947, 2965, 3011.

5b: A procedure analogous to that used to prepare **5a** was used, but starting from **3b** (1.0 mmol, 0.21 g).Yield: 88% (0.30 g, 0.88 mmol). Anal. Calcd for $C_{10}B_9H_{32}N_3Ti_1$: C, 35.37; H, 9.50; N, 12.38. Found: C, 35.02; H, 9.40; N, 12.13. ^{11}B NMR (96.3 MHz, $CDCl_3$): δ −26.26 (1B), −14.18 (2B), −10.49 (3B), −7.01 (2B), 0.43 (1B). IR spectrum (KBr pellet, cm^{-1}): ν(B−H) 2494, 2540, ν(C−H) 2944, 2993.

6a: A procedure analogous to that used to prepare **5a** was used, but starting from **3a** (1.0 mmol, 0.19 g). Yellow crystalline solid. Yield: 77% (0.32 g, 0.77 mmol). Anal. Calcd for $C_{11}B_9H_{37}N_4Zr_1$: C, 31.92; H, 9.00; N, 13.53. Found: C, 32.17; H, 8.87; N, 13.67. ^{11}B NMR (96.3 MHz, $CDCl_3$): δ −26.06 (1B), −16.94 (2B), −12.66 (3B), −9.13 (1B), −7.58 (1B), −1.21 (1B). IR spectrum (KBr pellet, cm^{-1}): ν(B−H) 2538, ν(C−H) 2845, 2963, ν(N−H) 3167.

6b: A procedure analogous to that used to prepare **5a** was used, but starting from **3b** (1.0 mmol, 0.21 g). Yield: 82% (0.35 g, 0.82 mmol). Anal. Calcd for $C_{12}B_9H_{39}N_4Zr_1$: C, 33.68; H, 9.18; N, 13.09. Found: C, 33.48; H, 8.89; N, 12.77. ^{11}B NMR (96.3 MHz, $CDCl_3$): δ −31.03 (1B), −31.03 (1B), −26.62 (1B), −18.06 (1B), −13.07 (2B), −11.60 (2B), −7.91 (1B), −2.61 (1B). IR spectrum (KBr pellet, cm^{-1}): ν(B−H) 2527, ν(C−H) 2775, 2874, 2961, ν(N−H) 3182.

Preparation of Compound 3 from Compound 5. Complex **5a** (0.33 g, 1.0 mmol) was dissolved in CH_2Cl_2 (15 mL), and then an excess amount of Me_3SiCl (3.3 equiv) was added. The resulting mixture was stirred for 1 h, after which all volatiles were removed under vacuum and the residue was washed with pentane three times. Removal of the volatiles under vacuum provided the final crude product. Extraction of the residue with toluene (20 mL) followed by concentration to approximately half its volume and cooling to −10 °C provided pure complex **4a** as a red solid. Yield: 75% (0.23 g, 0.75 mmol). For **4b**, a procedure similar to that described for **4a** was employed, but with the following quantities: compound **5b** (0.34 g, 1.0 mmol). Yield: 71% (0.23 g, 0.71 mmol).

Preparation of $(Dcab^N)_2M$ (M = Ti, 7; Zr, 8; Hf, 9). To a slurry solution of the dianion of **3a** (0.38 g, 2.0 mmol) in 20 mL of toluene, precooled to −78 °C, was added $TiCl_4$ (0.19 g, 1.0 mmol) at −78 °C, and the resulting mixture was stirred for 30 min. The resultant red mixture was allowed to warm to 25 °C and stirred for 2 h. ^{1}H NMR spectroscopy demonstrated that **7** was formed after 5 min at room temperature. The mixture was concentrated to ca. 5 mL and cooled to −10 °C, giving a red precipitate of **7**, which was filtered and dried under vacuum. Yield: 47% (0.20 g, 0.47 mmol). Anal. Calcd for $C_{10}B_{18}H_{36}N_2Ti_1$: C, 28.14; H, 8.50; N, 6.56. Found: C, 28.01, H, 8.33, N, 6.44. ^{11}B NMR (96.3 MHz, $CDCl_3$): δ −10.70 (1B), −7.59 (1B), −5.74 (1B), −4.37 (1B), −2.03 (1B), 3.53 (1B), 6.24 (1B), 9.06 (1B), 28.47 (1B). IR spectrum (KBr pellet, cm^{-1}): ν(B−H) 2537, ν(C−H) 2850, 2919, 2958.

8: A procedure analogous to that used to prepare **7** was used, but starting from $ZrCl_4$ (0.27 g, 1.0 mmol) in toluene. Crystals suitable for X-ray diffraction analysis were obtained from a saturated toluene solution at −10 °C. Yield: 55% (0.26 g, 0.55 mmol). Anal. Calcd for $C_{10}B_{18}H_{36}N_2Zr_1$: C, 25.54, H, 7.72, N, 5.96. Found: C, 25.42; H, 7.59; N, 5.83. ^{11}B NMR (96.3 MHz, $CDCl_3$): δ −13.23 (1B), −10.03 (1B), −7.84 (1B), −4.81 (1B), −3.35 (1B), −0.25 (2B), 2.84 (1B), 12.11 (1B). IR spectrum (KBr pellet, cm^{-1}): ν(B−H) 2526, ν(C−H) 2932, 2995, 3024.

9: A procedure analogous to that used to prepare **7** was used, but starting from $HfCl_4$ (0.35 g, 1.0 mmol) in toluene. Complex **9** was recrystallized from toluene at −10 °C. Yield: 41% (0.23 g, 0.41 mmol). Anal. Calcd for $C_{10}B_{18}H_{36}N_2Hf_1$: C, 21.55; H, 6.51; N, 5.03. Found: C, 21.40; H, 6.38; N, 4.89. ^{11}B NMR (96.3 MHz, $CDCl_3$): δ −23.17 (1B), −15.51 (1B), −12.83 (1B), −11.13 (1B),

Table 4. X-ray Crystallographic Data and Processing Parameters for Compounds 2a, 5a, 5b, 6a, 8·C_7H_8, 11·C_6H_6, and 12·C_6H_6

	2a	**5a**	**5b**	**6a**	**8**·C_7H_8	**11**·C_6H_6	**12**·C_6H_6
formula	$C_9B_9H_{31}N_2$	$C_9B_9H_{30}N_3Ti$	$C_{10}B_9H_{32}N_3Ti$	$C_{11}B_9H_{37}N_4Zr$	$C_{17}B_{18}H_{44}N_2Zr$	$C_{23}B_9H_{34}NO_2Ti$	$C_{25}B_9H_{38}NO_2Ti$
fw	264.65	325.52	339.55	413.96	562.34	501.69	529.75
cryst syst	orthorhombic	orthorhombic	monclinic	triclinic	monoclinic	monoclinic	monoclinic
Z, space group	4, $P2_12_12_1$	4, *Pnma*	4, $P2_1/n$	2, $P\bar{1}$	4, $P2_1/c$	2, $P2_1/m$	4, $P2_1/c$
a/Å	10.5791(7)	17.510(2)	9.4288(1)	9.2199(8)	18.0299(1)	7.6576(3)	11.7288(7)
b/Å	11.3215(2)	13.1509(2)	14.8273(1)	9.2777(8)	10.4035(6)	20.2081(9)	11.7786(7)
c/Å	14.9539(9)	8.0442(1)	13.6057(1)	13.8417(1)	16.090(2)	9.4735(4)	22.3691(1)
V/Å^3	1791.0(3)	1852.3(4)	1901.2(3)	1078.3(2)	2998.3(5)	1361.8(1)	3088.5(3)
μ/mm^{-1}	0.049	0.453	0.445	0.511	0.380	0.336	0.300
cryst size/mm	0.5 × 0.5 × 0.4	0.25 × 0.15 × 0.1	0.25 × 0.15 × 0.1	0.3 × 0.15 × 0.15	0.5 × 0.4 × 0.4	0.18 × 0.16 × 0.14	0.2 × 0.17 × 0.09
no. of reflns collected/unique	2006/2006	12 979/2400	13 684/4727	8012/5315	6093/5868	18 785/3476	31 249/7664
no. of reflns obsd [$I > 2\sigma(I)$]	756	943	2920	4116	3853	2568	2102
R(int)	0.0000	0.1718	0.0643	0.08	0.0336	0.0573	0.1214
R [$I > 2\sigma(I)$], wR_2	0.1164, 0.2728	0.0843, 0.2190	0.0495, 0.1064	0.0388, 0.0855	0.0377, 0.1017	0.0492, 0.1142	0.0811, 0.2134
R (all data), wR_2	0.2925, 0.3492	0.2196, 0.3081	0.1013, 0.1247	0.0556, 0.0894	0.0726, 0.1150	0.1027, 0.1472	0.2357, 0.3167

Table 5. Selected Interatomic Distances (Å) for Compounds 5a, 5b, 6a, 8·C_7H_8, 11·C_6H_6, and 12·C_6H_6

	5a	**5b**	**6a**	**8**·C_7H_8	**11**·C_6H_6	**12**·C_6H_6	CGC[c]
M−C1	2.349(7)	2.385(2)	2.617(2)	2.467(3), 2.469(3)	2.332(3)	2.327(5)	
M−C2	2.386(7)	2.359(3)	2.655(3)	2.473(4), 2.497(4)	2.353(3)	2.343(6)	
M−B9	2.434(8)	2.426(3)	2.609(3)	2.573(5), 2.592(5)	2.388(3)	2.362(6)	
M−B10	2.434(8)	2.456(3)	2.577(3)	2.593(5), 2.580(4)	2.388(3)	2.395(6)	
M−B11	2.386(7)	2.484(2)	2.567(3)	2.504(3), 2.489(4)	2.353(3)	2.344(6)	
M−$DCab_{(centr)}$	1.931	1.950	2.180	2.077, 2.081	1.881	1.870	2.030
M−N1	2.220(7)	2.255(2)	2.579(2)	2.488(3), 2.460(3)	2.178(3)	2.190(4)	1.907(3)
M−N2	1.893(5)	1.900(2)	2.054(2)				
M−N3	1.893(5)	1.901(2)	2.033(2)				
M−N4			2.450(2)				
M−O1					1.779(2)	1.782(3)	
M−O2					1.779(2)	1.783(4)	
M−Cl1							2.2635(11)
M−Cl2							2.2635(11)

Table 6. Selected Interatomic Angles (deg) for Compounds 5a, 5b, 6a, 8·C_7H_8, 11·C_6H_6, and 12·C_6H_6

	5a	**5b**	**6a**	**8**·C_7H_8	**11**·C_6H_6	**12**·C_6H_6	CGC[c]
$DCab_{(centr)}$−C1−C3	147.27	146.99	151.02	151.37, 151.95	146.23	146.03	
N1−M−$DCab_{(centr)}$	99.39	98.22	86.85	93.47, 93.43	99.97	99.85	107.6
C1−C3−N1	106.9(7)	106.57(19)	109.9(2)	108.3(3), 108.1(3)	104.9(3)	105.2(4)	
N2−M−N3	102.5(3)	99.77(9)	116.39(9)				
O1−M−O2					102.4(1)	103.3(2)	
Cl1−M−Cl2							102.97(7)

−9.26 (1B), −4.50 (1B), −1.75 (1B) 1.87 (1B) 9.18 (1B). IR spectrum (KBr pellet, cm^{-1}): ν(B−H) 2539, ν(C−H) 2920, 2992, 3036.

Preparation of ($Dcab^N$)Ti(O^iPr)$_2$, 10. To a stirred solution of **3a** (0.19 g, 1 mmol) in toluene (20 mL) was added 0.28 g of Ti(O^iPr)$_4$ (1 mmol). The mixture was heated at reflux for 12 h. The solvent was then removed under vacuum, and the residue was washed with hexane three times. Removal of the volatiles provided the final crude product, which was further purified from toluene at −35 °C to provide pure complex **10** as an orange solid. Yield: 70% (0.25 g, 0.7 mmol). Anal. Calcd for $C_{11}B_9H_{32}N_1O_2Ti_1$: C, 37.16; H, 9.07; N, 3.94. Found: C, 37.12; H, 9.09; N, 3.93. ^{11}B NMR (96.3 MHz, $CDCl_3$): δ −43.48 (1B), −25.81 (2B), −17.06 (3B), −11.05 (2B), −0.835 (1B). IR spectrum (KBr pellet, cm^{-1}): ν(B−H) 2532, ν(C−H) 2853, 2922.

Preparation of ($Dcab^N$)Ti(OC_6H_5)$_2$, 11. A representative procedure is as follows. Compound **5a** (0.33 g, 1.0 mmol) was dissolved in toluene (15 mL), and then an excess amount of C_6H_5-OH (2.1 equiv) was added. The reaction mixture was maintained at 80 °C for 30 min. Removal of the volatiles provided the final crude product. Extraction of the residue with benzene (10 mL), followed by concentration to approximately half its volume, resulted in crystallization of a pure orange solid. Yield: 85% (0.36 g, 0.85 mmol). Anal. Calcd for $C_{17}B_9H_{28}N_1O_2Ti_1$: C, 48.20; H, 6.66; N, 3.31. Found: C, 48.09; H, 6.68; N, 3.32. ^{11}B NMR (96.3 MHz, $CDCl_3$): δ −2.74 (1B), −14.77 (2B), −8.30 (2B), −4.56 (3B), 9.14 (1B). IR spectrum (KBr pellet, cm^{-1}): ν(B−H) 2536, ν(C−H) 2961, 3030, 3055.

Preparation of ($Dcab^N$)Ti[O-(2-MeC_6H_4)]$_2$, 12. A procedure similar to that described above for **11** was employed, but with the following quantities: compound 2-MeC_6H_4OH (2.1 equiv). Yield: 80% (0.36 g, 0.80 mmol). Anal. Calcd for $C_{19}B_9H_{32}N_1O_2Ti_1$: C, 50.53; H, 7.14; N, 3.10. Found: C, 50.44; H, 7.13; N, 3.09. ^{11}B NMR (96.3 MHz, $CDCl_3$): δ −20.78 (2B), −14.37 (2B), −6.20 (3B), 9.50 (2B). IR spectrum (KBr pellet, cm^{-1}): ν(B−H) 2540, ν(C−H) 2913, 2955.

Crystal Structure Determination. Crystals of **2a**, **5a**, **5b**, **6a**, **8**·C_7H_8, **11**·C_6H_6, and **12**·C_6H_6 were obtained from toluene, sealed in glass capillaries under argon, and mounted on the diffractometer. Preliminary examination and data collection were performed using a Bruker SMART CCD detector system single-crystal X-ray diffractometer equipped with a sealed-tube X-ray source (40 kV × 50 mA) using graphite-monochromated Mo Kα radiation (λ = 0.71073 Å). Preliminary unit cell constants were determined with a set of 45 narrow-frame (0.3° in ω) scans. The double-pass method of scanning was used to exclude any noise. The collected frames were integrated using an orientation matrix determined from the narrow-frame scans. The SMART software package was used for data collection, and SAINT was used for frame integration.[25a] Final cell constants were determined by a global refinement of *xyz* centroids of reflections harvested from the entire data set. Structure solution and refinement were carried out using the SHELXTL-PLUS software package.[25b] The *R* factors for **2a** and **12** are rather high. **2a** is presumably responsible for the poor crystal quality and the large thermal vibrations of B3, B8, C4, and C7 because the X-ray intensity data were collected at room temperature. The *R* factor was slightly large in **12**, and the C8, C9, C10, and C11 atoms in the phenyl ring were disordered over two positions. When the unprimed and primed atoms in the phenyl ring shown in Figure 7 were refined anisotropically with a respective identical occupancy, the C8, C9, C10, and C11 atoms were disordered again over two positions. Therefore, they were refined isotropically in order to avoid unusual displacement parameters. The site-occupancies were refined by using PART instruction in SHELXL-97, and finally they reached 0.28(2) and 0.72(2), respectively. Some of bond lengths and angles in the two rings differ considerably from the normal values owing to the disordering. Detailed information is listed in Tables 5 and 6.

Ethylene Homopolymerization. Cyclohexane (300 mL) and mMAO-7 were introduced to a thoroughly dried 500 mL autoclave reactor, and the reactor was heated to 140 °C. Specific amounts of catalyst and [Ph_3C][B(C_6F_5)$_4$] toluene solution were added through a catalyst injector, and the reactor was pressurized with ethylene up to 30 kg/cm^2 to start polymerization. During polymerization, the reactor pressure stayed constant by continuously feeding ethylene. After 10 min, the reactor was cooled to 55 °C and degassed, and 5 mL of acidic ethanol was added to stop polymerization. The solution was then poured into 1500 mL of ethanol, and the resultant polymer was recovered by filtration and dried *in vacuo* at 70 °C for 12 h.

Acknowledgment. This work was supported by the SRC program of MOST/KOSEF through the Center for Intelligent Nano-Bio Materials at Ewha Womans University (Grant R11-2005-008-00000-0) and the Korea Research Foundation Grant

---

(25) (a) *SMART* and *SAINT*; Bruker Analytical X-ray Division: Madison, WI, 2002. (b) Sheldrick, G. M. *SHELXTL-PLUS* Software Package; Bruker Analytical X-ray Division: Madison, WI, 2002.

funded by the Korean Government MOEHRD (KRF-2005-070-C00072) and MOCIE (Contract No. 10016495).

Supporting Information Available: Tables giving crystallographic data for the structures of **2a**, **5a**, **5b**, **6a**, **8**·C_7H_8, **11**·C_6H_6, and **12**·C_6H_6 reported in this paper. This material is available free of charge via the Internet at http://pubs.acs.org.

OM0701569